An Artificial Amino Acid, 4-Iodo-L-*meta*-Tyrosine: Biodistribution and Excretion via Kidney

Naoto Shikano, MS[1]; Keiichi Kawai, PhD[2]; Leo Garcia Flores II, MD, PhD[3]; Ryuichi Nishii, MD, PhD[3]; Nobuo Kubota, PhD[1]; Nobuyoshi Ishikawa, MD, PhD[1]; and Akiko Kubodera, PhD[4]

[1]Department of Radiological Sciences, Ibaraki Prefectural University of Health Sciences, Ibaraki, Japan; [2]School of Health Sciences, Faculty of Medicine, Kanazawa University, Ishikawa, Japan; [3]Department of Radiology, Miyazaki Medical College, Miyazaki, Japan; and [4]Faculty of Pharmaceutical Sciences, Science University of Tokyo, Tokyo, Japan

We evaluated the use of radiolabeled 4-iodo-L-*meta*-tyrosine as an amino acid transport marker. The pharmacologic features of this compound, particularly the biodistribution and excretion, were examined by conducting in vivo and in vitro studies using 4-^{125}I-iodo-L-*meta*-tyrosine (4-^{125}I-*m*Tyr). Results obtained for L-^{14}C-Tyr and 3-^{125}I-iodo-α-methyl-L-tyrosine (^{125}I-IMT) were used for comparison. **Methods:** In vivo biodistribution studies of 4-^{125}I-*m*Tyr were performed in male ddY mice. Urinary excretion of 4-^{125}I-*m*Tyr and ^{125}I-IMT with administration of probenecid was studied. Local distribution of 4-^{125}I-*m*Tyr and ^{125}I-IMT in kidney was visualized by autoradiography. We performed metabolite analysis of 4-^{125}I-*m*Tyr in mice. For in vitro studies, reabsorption mechanisms of 4-^{125}I-*m*Tyr were compared with those of ^{125}I-IMT and the parent L-^{14}C-Tyr using superconfluent monolayers of the porcine kidney epithelial cell line LLC-PK$_1$ in medium containing inhibitor (L-Tyr, D-Tyr, and 2,4-dinitrophenol), in Na^+-free medium, and at 4°C. **Results:** 4-^{125}I-*m*Tyr demonstrated high accumulation in the pancreas and kidney and comparable brain uptake to that of ^{125}I-IMT. Blood clearance of 4-^{125}I-*m*Tyr was faster than that of ^{125}I-IMT. Three hours after administration, >70% of 4-^{125}I-*m*Tyr was excreted via the urine, whereas <5% was found in the feces. Renal autoradiography revealed moderate accumulation of 4-^{125}I-*m*Tyr and high accumulation of ^{125}I-IMT in the renal cortex. Probenecid further reduced accumulation of 4-^{125}I-*m*Tyr and ^{125}I-IMT in the kidney as well as urinary excretion. At 30 min after tracer injection, intact free 4-^{125}I-*m*Tyr accounted for >98.1% of the total present in kidney and >96.3% in urine. Protein incorporation was not observed. Uptake of 4-^{125}I-*m*Tyr into LLC-PK$_1$ cell monolayers was remarkably reduced by 5 mmol/L L-Tyr (4.6%) and incubation at 4°C (15.6%) but was reduced by 5 mmol/L D-Tyr (50.0%). L-^{14}C-Tyr and ^{125}I-IMT showed similar results; however, uptake of ^{125}I-IMT was enhanced by 0.1 mmol/L 2,4-dinitrophenol (165.1%), an inhibitor of generation of energy-rich phosphates. **Conclusion:** The artificial amino acid 4-^{125}I-*m*Tyr demonstrated high metabolic stability, rapid blood clearance, rapid urinary excretion, and similar biodistribution to other radiolabeled L-Tyr analogs. 4-^{125}I-*m*Tyr can be a competitive substrate of L-Tyr reabsorption. However, 4-^{125}I-*m*Tyr demonstrates different pharmacologic features than those of ^{125}I-IMT, particularly in renal handling. 4-^{125}I-*m*Tyr may potentially be applied as a new amino acid transport marker.

Key Words: amino acid transport; artificial amino acid; LLC-PK$_1$; 4-iodo-L-*meta*-tyrosine; SPECT

J Nucl Med 2003; 44:625–631

We recently studied the feasibility of iodinated L-*meta*-tyrosine (I-L-*m*Tyr) for measuring amino acid transport in the brain and pancreas (*1*). The results indicated that I-L-*m*Tyr is resistant to deiodination and accumulates in the brain. This was thought to be because the L-amino acids penetrate the brain and the hydroxy group at position 3 increases the metabolic stability (*1*). According to the method of Adams et al. (*2*), radioiodination of L-*m*Tyr results in 2 major geometric isomers, 6-iodo- and 4-iodo-L-*m*Tyr (6-I-*m*Tyr, 4-I-*m*Tyr). We separated these isomers using high-performance liquid chromatography (HPLC) (*3*). The new radiopharmaceutical 6-I-*m*Tyr was reported to be useful in assessing cerebral amino acid transport mechanisms and quantifying metabolically active dihydroxyphenylalanine (DOPA) decarboxylase (*3*).

In this article, we present the pharmacologic features of the artificial amino acid 4-^{125}I-iodo-L-*meta*-tyrosine (4-^{125}I-*m*Tyr) (Fig. 1) (*2,3*). We investigated the biodistribution and excretion and conducted metabolite analysis of 4-^{125}I-*m*Tyr in mice. The renal handling of this compound was studied in detail because most of the 4-^{125}I-*m*Tyr proved to be excreted via kidney. Renal accumulation of 4-^{125}I-*m*Tyr and 3-^{125}I-iodo-α-methyl-L-tyrosine (^{125}I-IMT) was visualized by autoradiography. Furthermore, the carrier systems related to reabsorption of the apical membrane involved in 4-^{125}I-*m*Tyr transport were examined using superconfluent monolayers of a porcine kidney epithelial cell line (LLC-PK$_1$) on plastic dishes (*4,5*). The results were compared with the data for the parent Tyr and ^{125}I-IMT. The LLC-PK$_1$ model has been used extensively for analyzing several functions of the proximal tubules (*6–10*). In this experimental model, LLC-PK$_1$ forms an oriented monolayer with tight junctions on the plastic surface and exhibits reabsorption of electrolytes and

Received May 14, 2002; revision accepted Nov. 14, 2002.

For correspondence or reprints contact: Naoto Shikano, MS, Department of Radiological Sciences, Ibaraki Prefectural University of Health Sciences, 4669-2 Ami, Ami-machi, Inashiki-gun, Ibaraki 300-0394, Japan.

E-mail: sikano@ipu.ac.jp

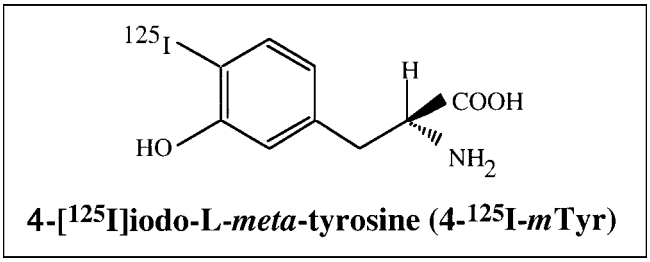

FIGURE 1. Chemical structure of 4-^{125}I-*m*Tyr.

some nutrients via the microvilli of the apical membrane, which are in contact with the uptake solution (*5*).

We also discuss the clinical perspectives of using 4-^{125}I-*m*Tyr on the basis of this investigation and earlier studies (*1*). To the best of our knowledge, this is the first detailed study and pharmacologic characterization of 4-I-*m*Tyr.

MATERIALS AND METHODS

Preparation of 4-^{125}I-*m*Tyr

Reagent-grade chemicals were used in this investigation (Kanto Chemical Co., Tokyo, Japan). DL-*m*Tyr was acquired from Sigma-Aldrich Japan K.K. (Tokyo, Japan) and was separated by HPLC using a chiral column (Crownpak CR(−), 4 × 150 mm; Daicel Chemical Industries, Tokyo, Japan). ^{125}I-NaI was obtained from Amersham Pharmacia Biotech U.K. (Buckinghamshire, U.K.). The conventional chloramine-T method was used to prepare 4-^{125}I-*m*Tyr, as reported (*2*). Chloramine-T (Sigma-Aldrich Japan) at a concentration of 1.0×10^{-3} mol/L in 10 μL 0.05 mol/L phosphate buffer (pH 8.5) was added to a mixture of L-*m*Tyr (100 μL at 1.0×10^{-3} mol/L) and carrier-free ^{125}I-NaI (3.7–7.4 MBq) in 35 μL 0.4 mol/L phosphate buffer (pH 8.5). The resulting solution was allowed to stand for 30 min, and 10 μL of 1.0×10^{-3} mol/L sodium metabisulfite in 0.05 mol/L phosphate buffer (pH 8.5) were added.

Geometric isomer separation by HPLC was then performed using a Nova-Pak C_{18} column (3.9 × 300 mm; Waters, Milford, MA; eluent, 0.02 mol/L potassium acetate:ethanol = 90:1; flow rate, 0.5 mL/min; retention time: 4-isomer, 17–20 min; I^-, 4–5 min; cold *m*Tyr, 5–7 min). Labeling efficiency and radiochemical purity were studied using silica gel thin-layer chromatography ([TLC] catalog number Art. 5553; Merck, Darmstadt, Germany) with 2 solvent systems, methanol:acetic acid = 100:1 (R_f value: 4-^{125}I-*m*Tyr, 0.50; I^-, 0.80) and methanol:10% ammonium acetate = 10:1 (R_f value: 4-^{125}I-*m*Tyr, 0.55; I^-, 0.80). Solvent exchange was performed using saline.

As references, L-^{14}C(U)-tyrosine (L-^{14}C-Tyr; American Radiolabeled Chemicals Co., St. Louis, MO), a labeled natural amino acid, was used as the gold standard. ^{125}I-IMT was prepared using the method reported previously (*11*,*12*).

Biodistribution and Urinary Excretion in Mice

The ethical committees of all affiliated universities approved all animal experiments in this study. Male ddY mice (n = 5; weight, 30 g) were administered 0.1 mL 4-^{125}I-*m*Tyr (1.11 kBq) by injection into the tail vein. For inhibition studies, probenecid (50 mg/kg body weight) was preadministered through the tail vein 10 min before injection of 4-^{125}I-*m*Tyr (*13*). Urine and feces were collected at various time intervals after administration. Mice were anesthetized with ether and killed by cardiac puncture. Radioactivity of urine and various organs was measured using an ARC-1000M well-type scintillation counter (Aloka, Tokyo, Japan).

In Vivo Stability

For metabolite analysis, male ddY mice (n = 5; weight, 30 g) were injected with 0.1 mL 4-^{125}I-*m*Tyr (50 kBq) into the tail vein. After 30 min, mice were anesthetized with ether and killed by cardiac puncture. An aliquot of tissue was homogenized, and the 5% trichloroacetic acid–precipitated fraction was trapped on a GC-50 glass filter (Advantec MFS, Inc., Dublin, CA) to facilitate measurement of the radioactivity incorporated into the protein. Tissue supernatant was separated by silica gel TLC (catalog number Art. 5553; Merck) using the following solvent systems: methanol:acetic acid = 100:1 (R_f value: 4-^{125}I-*m*Tyr, 0.5; I^-, 0.80) and methanol:10% ammonium acetate = 10:1 (R_f value: 4-^{125}I-*m*Tyr, 0.55; I^-, 0.80).

In Vivo Autoradiography

For autoradiography, 0.1 mL 4-^{125}I-*m*Tyr or ^{125}I-IMT (670 kBq) was injected into the tail vein of male ddY mice (n = 4; weight, 30 g). After 5 min, mice were killed by inspiration of excess ether. The kidney was placed in carboxymethylcellulose embedding medium (Nacalai, Kyoto, Japan) and then frozen at −15°C for at least 12 h. A Handex cryostat microtome (Shiraimatsu, Osaka, Japan) was used to cut 20-mm coronal sections from posterior to anterior. Sections were then dried at −15°C for another 24 h. Tissue slices were left in contact with BAS-TR2040 imaging plates (Fuji Photo Film, Kanagawa, Japan) for 24 h. Images were processed using a BAS 2000 Bio-Imaging Analyzer (Fuji Photo Film).

In Vitro Measurement of Reabsorption

Cell line studies were performed as described by Saito et al. (*5*). Briefly, LLC-PK_1 cells were obtained from Dainippon Pharmaceutical Co. (Osaka, Japan; catalog number 09-1392) and were cultured on plastic dishes (Falcon; Becton Dickinson, Lincoln Park, NJ) in Dulbecco's modified Eagle's medium (Sigma Chemical Co., St. Louis, MO), supplemented with 10% fetal calf serum (Equitech-Bio Inc., Ingram, TX) without antibiotics, in an atmosphere of 5% CO_2:95% air at 37°C. Subculturing was conducted every 7 d using 0.02% ethylenediaminetetraacetic acid and 0.05% trypsin. In this study, cells were used between the 220th and 235th passages.

For uptake studies, LLC-PK_1 cells were seeded on 60-mm dishes at a cell density of 5×10^5 cells per dish in 5 mL complete medium and were used on the 6th and 7th days after inoculation. Uptake was measured in LLC-PK_1 cell monolayers grown on 60-mm plastic culture dishes. The incubation medium comprised 145 mmol/L NaCl, 3 mmol/L KCl, 1 mmol/L $CaCl_2$, 0.5 mmol/L $MgCl_2$, and 5 mmol/L 2-hydroxyethylpiperazine-*N*′-2-ethanesulfonic acid, with a final pH of 7.4. In the Na^+-dependence study, NaCl was replaced with the same concentration of choline-Cl. After removal of culture medium, each dish was washed once with 5 mL incubation medium for 10 min at 37°C. Cells were then incubated with 2 mL incubation medium containing no-carrier-added 4-^{125}I-*m*Tyr or L-^{14}C-Tyr for the specified periods at 37°C, and in the temperature dependence study, at 4°C.

For the inhibition study, L-Tyr, D-Tyr, probenecid, and 2,4-dinitrophenol (2,4-DNP) were added to give final concentrations of 5.0 mmol/L (*14*), 5.0 mmol/L (*14*), 1 mmol/L (*15*), and 0.1 mmol/L (*16*), respectively. Cells were incubated for 5 min at 37°C

with 1.11 kBq of no-carrier-added 4-^{125}I-*m*Tyr or L-^{14}C-Tyr (American Radiolabeled Chemicals).

Thereafter, media were aspirated, and monolayers were rinsed twice rapidly using 5 mL ice-cold incubation medium. Cells were solubilized in 1.5 mL 1N NaOH, and the radioactivity of each aliquot was counted. Radioactivity associated with solubilized cells was determined using an ARC-1000M well-type scintillation counter (Aloka) and an LS6500 liquid scintillation counter (Beckman Instruments, Fullerton, CA).

Statistical Analysis

Data are expressed as mean ± SD of 3-5 measurements and each experiment was performed in duplicate. Results were analyzed using the Student *t* test. $P < 0.05$ was considered statistically significant.

RESULTS

Preparation of 4-^{125}I-*m*Tyr

Labeling of L-*m*Tyr yielded 4-^{125}I-*m*Tyr with labeling efficiency exceeding 80%. After purification, no-carrier-added 4-^{125}I-*m*Tyr with radiochemical purities exceeding 95% was obtained.

Biodistribution and Urinary Excretion in Mice

Table 1 summarizes the biodistribution of 4-^{125}I-*m*Tyr in healthy mice. The observed accumulation of 4-^{125}I-*m*Tyr in the pancreas was higher than that in the kidney. Accumulation of 4-^{123}I-*m*Tyr in mouse kidney cortex was approximately 80% lower than that of ^{125}I-IMT in terms of percentage injected dose/gram of tissue (%ID/g tissue) (Tables 1 and 2; Fig. 2B).

As shown in Figure 2A, rapid clearance of 4-^{125}I-*m*Tyr from the blood was observed. Although the clearance of 4-^{125}I-*m*Tyr was faster than that of ^{125}I-IMT in all organs studied, organ-to-blood ratios were similar with the exception of the kidney.

Urinary excretion of 4-^{125}I-*m*Tyr was rapid and delayed by probenecid administration (Fig. 3). These results demonstrate that secretion of 4-^{125}I-*m*Tyr is competitively inhibited by probenecid.

TABLE 1
Biodistribution of 4-^{125}I-*m*Tyr in Male ddY Mice

Biodistribution	5 min	15 min	30 min
Blood*	3.72 ± 0.40	1.56 ± 0.36	0.45 ± 0.09
Brain	0.61 ± 0.16	0.47 ± 0.07	0.32 ± 0.08
Pancreas	25.44 ± 1.85	14.03 ± 3.69	2.00 ± 0.57
Liver	4.31 ± 0.51	1.80 ± 0.42	0.64 ± 0.16
Stomach	1.24 ± 0.22	1.05 ± 0.37	2.82 ± 2.27
Intestine	2.26 ± 0.29	1.03 ± 0.26	0.56 ± 0.06
Kidney	23.77 ± 4.89	12.89 ± 9.53	4.24 ± 1.92
Heart	2.51 ± 0.33	1.42 ± 0.34	0.92 ± 0.36
Lung	3.76 ± 0.52	1.90 ± 0.41	0.74 ± 0.14
Spleen	4.04 ± 0.64	2.35 ± 1.05	0.54 ± 0.17

*%ID/mL blood (n = 5 mice).
All data except blood are expressed as %ID/g tissue, mean ± 1 SD.

TABLE 2
Biodistribution of ^{125}I-IMT in Male ddY Mice

Biodistribution	5 min	15 min	30 min
Blood*	6.70 ± 1.44	3.12 ± 0.43	1.47 ± 0.08
Brain	0.58 ± 0.12	0.47 ± 0.08	1.05 ± 0.13
Pancreas	41.48 ± 5.16	25.84 ± 9.50	9.18 ± 1.89
Liver	4.63 ± 1.29	2.00 ± 0.15	0.93 ± 0.03
Stomach	4.31 ± 1.66	4.81 ± 1.39	2.93 ± 0.28
Intestine	5.08 ± 1.21	2.49 ± 0.65	0.91 ± 0.06
Kidney	102.62 ± 0.93	75.34 ± 15.74	24.05 ± 6.04
Heart	5.67 ± 2.16	3.10 ± 0.41	1.53 ± 0.08

*%ID/mL blood (n = 5 mice).
All data except blood are expressed as %ID/g tissue, mean ± 1 SD.

In Vivo Stability

Metabolite analysis revealed that intact free amino acid accounted for >98.11% ± 1.21% of the radioactivity in mouse kidney and >96.29% ± 3.10% in mouse urine. Protein incorporation of 4-^{125}I-*m*Tyr was not observed in mouse kidney. Furthermore, 4-^{125}I-*m*Tyr displayed high stability against deiodination because free iodine comprised only 0.17% ± 0.18% of radioactivity in the kidney and 3.50% ± 1.59% in urine.

In Vivo Autoradiography

Localization of 4-^{125}I-*m*Tyr and ^{125}I-IMT in the kidney is compared in Figure 4. At 5 min after administration, ^{125}I-IMT displayed substantial accumulation in the renal cortex, whereas 4-^{125}I-*m*Tyr showed only moderate accumulation. Most of the excreted 4-^{125}I-*m*Tyr was observed in the medulla. Probenecid inhibited the cortical accumulation of ^{125}I-IMT and 4-^{125}I-*m*Tyr.

In Vitro Measurement of Reabsorption

Time course analysis of 4-^{125}I-*m*Tyr uptake into LLC-PK$_1$ cell monolayers shows that steady-state levels were reached 25 min after starting incubation (data not shown). An incubation time of 5 min was chosen for the inhibition study. The results of inhibition studies of 4-^{125}I-*m*Tyr, ^{125}I-IMT, and L-^{14}C-Tyr uptake are shown in Figure 5. Significant

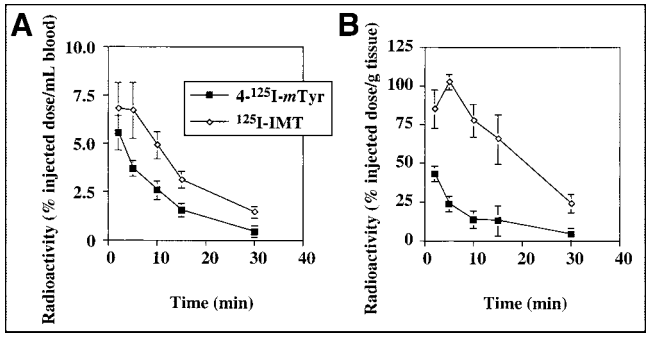

FIGURE 2. Biodistribution of 4-^{125}I-*m*Tyr compared with that of ^{125}I-IMT in mice. (A) Blood clearance. (B) Kidney radioactivity. Each bar represents mean ± SD of 5 animals.

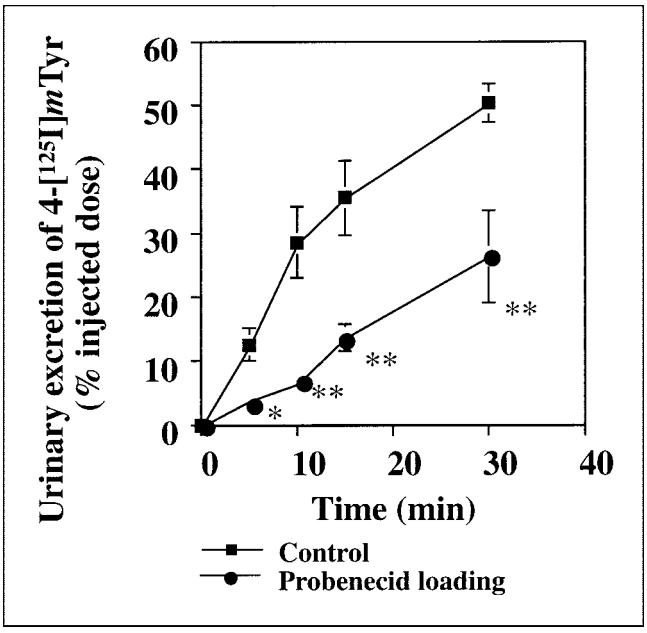

FIGURE 3. Urinary excretion of 4-^{125}I-*m*Tyr and effects of probenecid administration in mice. Control compared with probenecid administration. Each bar represents mean ± SD of 5 animals. *$P < 0.05$; **$P < 0.005$.

inhibition of 4-^{125}I-*m*Tyr uptake as well as inhibition of ^{125}I-IMT and L-^{14}C-Tyr uptake was noted with L-Tyr ($P < 0.01$). When compared with L-Tyr, D-Tyr had a smaller inhibitory effect on 4-^{125}I-*m*Tyr, ^{125}I-IMT, and ^{14}C-Tyr uptake. Replacing sodium with choline slightly reduced 4-^{125}I-*m*Tyr and L-^{14}C-Tyr transport into LLC-PK$_1$ cell monolayers.

Administration of 2,4-DNP slightly enhanced accumulation of 4-^{125}I-*m*Tyr and L-^{14}C-Tyr in LLC-PK$_1$ cell monolayers. However, 2,4-DNP remarkably enhanced the accumulation of ^{125}I-IMT.

As seen in Figure 5, transport of 4-^{125}I-*m*Tyr into LLC-PK$_1$ cell monolayers predominantly (87%) used the Na^+-independent system, with minor (13%) use of the Na^+-dependent system. Incubation at 4°C significantly decreased accumulation of 4-^{125}I-*m*Tyr, L-^{14}C-Tyr, and ^{125}I-IMT ($P < 0.01$). These compounds behaved similarly in inhibition studies.

DISCUSSION

Changes in amino acid transport are frequently observed in conditions such as cancer (*17*), neuropsychiatric diseases, and substance abuse (*18*). Some of the tyrosine derivatives used in positron emission CT (PET), such as *O*-(2-^{18}F-

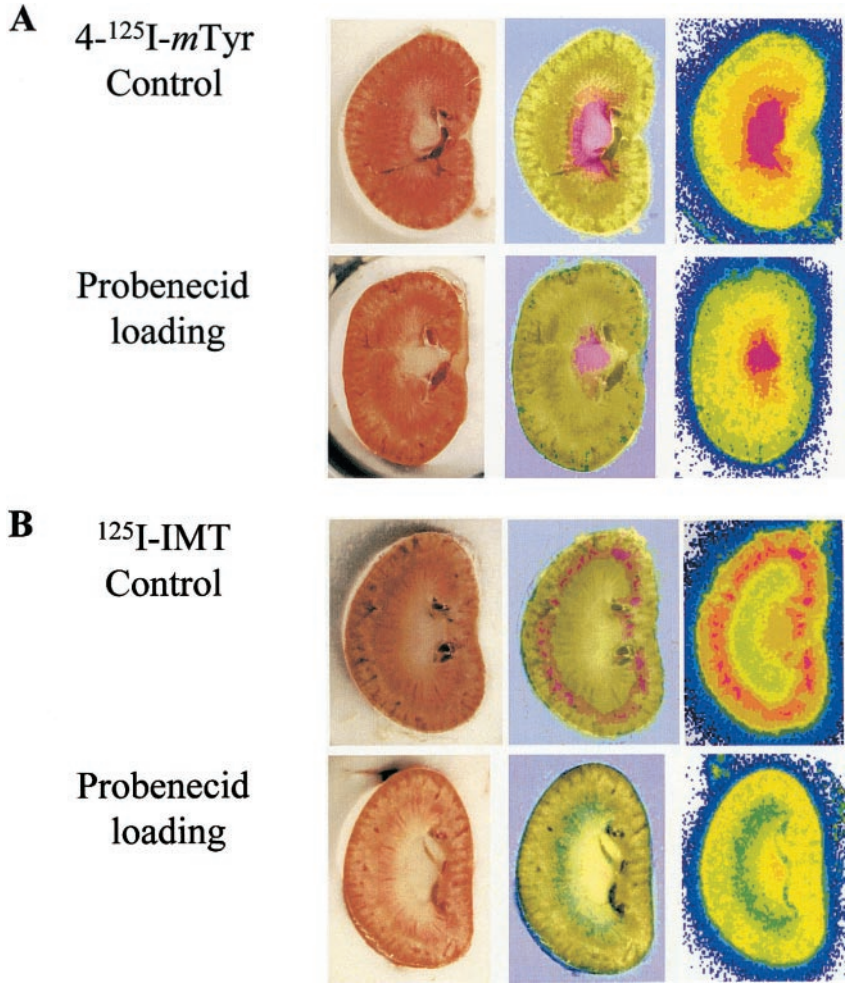

FIGURE 4. Comparison of 4-^{125}I-*m*Tyr (A) and ^{125}I-IMT (B) accumulation in mouse kidney with or without probenecid administration. (Left) Photograph. (Center) Superimposed. (Right) Autoradiograph.

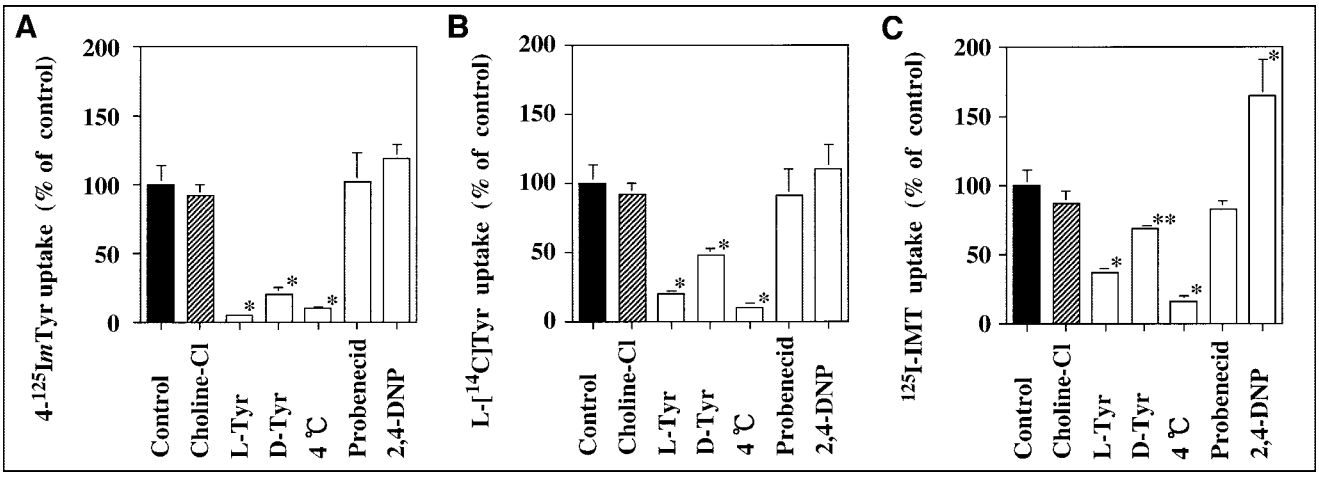

FIGURE 5. Effects of inhibitors on accumulation of 4-^{125}I-*m*Tyr (A) L-^{14}C(U)-Tyr (B), and ^{125}I-IMT (C) in LLC-PK$_1$ cell monolayers. Each column represents mean ± SD of 4 monolayers. *$P < 0.01$; **$P < 0.05$.

fluoroethyl)-L-tyrosine (^{18}F-FET) and 3-^{18}F-fluoro-α-methyl-L-tyrosine (^{18}F-FMT), and those used in SPECT, such as ^{123}I-IMT, are reportedly transported into cells via the neutral amino acid transport system (*19–21*). Of these compounds, ^{123}I-IMT has been successfully applied clinically for brain tumor imaging using SPECT (*22*); it has also been applied as an imaging agent to study brain and pancreas function (*11,12*).

In an attempt to develop a new amino acid transport marker, we opted to use SPECT, which is widely conducted with radioactive iodine. Because the phenol group of *m*Tyr provided a suitable site for labeling, direct electrophilic radioiodination was performed for preparation of 4-^{125}I-*m*Tyr. High labeling efficiency and specific activity of 4-^{125}I-*m*Tyr (no carrier added) can be obtained with the chloramine-T method. Radioactive iodine has the advantage of availability, low cost, and relatively long half-life. 4-^{125}I-*m*Tyr in saline was stable for 3 wk at 4°C.

The radioiodinated compound must be resistant to rapid breakdown by general metabolic pathways (*23*) because a complicated metabolic fate of a radioiodinated compound requires a complicated kinetic model for quantitative study. Furthermore, stability against deiodination is essential to prevent internal irradiation of organs that accumulate iodine, such as the thyroid and stomach. On the basis of the hypothesis that position 4 of the phenol hydroxyl group plays an important role in the substrate recognition of deiodinase, which reacts with 3-iodo-L-Tyr and 3,5-diiodo-L-Tyr, we hoped to increased resistance to iodination and to decrease renal accumulation by changing the position of the hydroxyl group of L-Tyr without α-methylation, as in ^{125}I-IMT. Furthermore, we hoped that 4-^{125}I-*m*Tyr would retain affinity for system L transport. The results of metabolic analysis of this study successfully demonstrated the high metabolic stability of 4-^{125}I-*m*Tyr, which is comparable to ^{125}I-IMT (*21*). 4-^{125}I-*m*Tyr was not a substrate for protein synthesis or deiodination. In the brain, no interaction with DOPA decarboxylase was observed during NSD-1015 inhibition studies (*3*). We believed that the hydroxy group at position 3 and the iodine at position 4 would result in the metabolic stability of 4-^{125}I-*m*Tyr (Fig. 1) (*1*).

Three hours after administration, >70% and <5% of intact compound was detected in the urine and feces, respectively. 4-^{125}I-*m*Tyr is predominantly excreted via the urinary tract, and hepatobiliary clearance does not appear to be substantially involved in excretion. Metabolic stability may be 1 factor contributing to the rapid renal excretion of the compound.

In the biodistribution study of 4-^{125}I-*m*Tyr (Table 1), rapid blood clearance, maximum tissue uptake, and prolonged retention in the organs were found, and this is comparable to the biodistribution of other amino acid analogs, such as ^{18}F-FET, ^{18}F-FMT, and ^{123}I-IMT (*19–21*). The higher accumulation in the pancreas is consistent with the characteristics of amino acid biodistribution.

The main difference between the biodistribution of 4-^{125}I-*m*Tyr and ^{125}I-IMT was the higher accumulation of ^{125}I-IMT in all organs studied (Tables 1 and 2). In particular, the accumulation of ^{125}I-IMT in kidney was about 5-fold higher than that of 4-^{125}I-*m*Tyr (Fig. 2B). Another α-methylated Tyr analog, ^{18}F-FMT, also exhibits high accumulation in the renal cortex (*24*). We propose that α-methylated Tyr analogs possess a higher affinity for accumulative renal organic anion secretion systems than non-α-methylated Tyr analogs, such as ^{18}F-FET (*19*) or 4-^{125}I-*m*Tyr. This is supported by the fact that probenecid, which is an organic anion secretion inhibitor in the kidney (*13,25*), markedly inhibits accumulative secretion of the α-methylated Tyr analog ^{125}I-IMT in the cortex of proximal tubule S2-like areas (Figs. 3 and 4). The actions of probenecid are largely confined to inhibition of organic anion transport across epithelial barriers (*13*). This is most important for the renal tubule, in which tubular secretion of many drugs and drug metabolites is inhibited (*13*). Furthermore, plasma protein binding of

both compounds was approximately 50% in our studies with rat (data not shown). Considering the results of urinary excretion inhibition analysis with probenecid, as shown in Figure 3, these data seem quite reasonable on the basis of the inhibited level of excretion. These results suggest different mechanisms of renal handling for 4-^{125}I-*m*Tyr and ^{125}I-IMT, and α-methylation could be the reason for this difference.

The results of recent studies have raised questions as to the nature of systems that mediate the membrane transport of Tyr analogs, such as ^{125}I-IMT, in cells of the renal cortex (*26*). After glomerular filtration, natural amino acids generally undergo intensive reabsorption and most natural amino acids are resorbed by S1 to S3 cells, and thus few amino acids are excreted (*27*). Figure 5 illustrates 1 possible solution to the above problem. In this experimental model, LLC-PK$_1$ exhibits reabsorption, because LLC-PK$_1$ comprises polar cells, with the apical side of monolayers contacting medium and the basolateral membrane on the wall of the culture dish (*5*). Figure 5 shows that reabsorption of both 4-^{125}I-*m*Tyr and L-Tyr was mediated by Na^+-independent as well as Na^+-dependent systems. Decreased accumulation of 4-^{125}I-*m*Tyr with incubation at 4°C suggests temperature-dependent carrier-mediated mechanisms for 4-^{125}I-*m*Tyr reabsorption. Probenecid exerted no effects on 4-^{125}I-*m*Tyr reabsorption.

Structural requirements for aromatic amino acid secretion and reabsorption in canines were investigated by Williams and Hang (*28,29*) using a series of Tyr analogs. It was concluded that the L-amino acids undergo secretion and reabsorption and that the L-configuration and amino group are required for reabsorption, whereas ring hydroxylation exerts little effect on resorptive transport (*29*). Results of excretion studies using probenecid in mice and similar studies in LLC-PK$_1$ provide evidence of secretion and reabsorption of 4-^{125}I-*m*Tyr. The results of our study agree with the above reports.

Several amino acid transport systems are known to mediate neutral amino acid transport in the kidney. Systems B^0 and $B^{0,+}$ are Na^+-dependent neutral amino acid transport systems, predominantly involved in the reabsorption of aromatic amino acids in the apical membrane of proximal tubule cells (*30–32*). System $b^{0,+}$ is a Na^+-independent transport system in the apical membrane of proximal tubule cells (*33*). This transport system is predominantly involved in the reabsorption of neutral and basic amino acids, including aromatic amino acids. The majority of A and ASC, Na^+-dependent neutral amino acid transport systems exist on the basal side of the membrane (*14*). System L is a Na^+-independent major nutrient transport system responsible for large neutral amino acids, including several essential amino acids (*34*). System L is exclusively located in the basolateral membranes (*14*). In addition to these transport systems, probenecid-competitive organic anion transport systems are believed to mediate ^{125}I-IMT as well as 4-^{125}I-*m*Tyr.

An interesting finding of this in vitro inhibition study in LLC-PK$_1$ is that 2,4-DNP, an inhibitor of energy-rich phosphate generation (*26*), caused a significant increase in ^{125}I-IMT uptake. Some of the energy-independent amino acid transport systems that exchange intracellular amino acids for extracellular amino acids in the apical side of the membrane of the proximal tubule cells are known (*30*). With the existence of an energy-dependent secretion system comprising energy-independent influx of ^{125}I-IMT and energy-dependent efflux, this phenomenon is well explained. 2,4-DNP could cause an increase in ^{125}I-IMT uptake by inhibiting efflux, and influx cannot be inhibited. However, 2,4-DNP caused a slight and statistically insignificant increase in 4-^{125}I-*m*Tyr and L-^{14}C-Tyr uptake.

Although few natural amino acids are excreted, rapid excretion of 4-^{125}I-*m*Tyr and ^{125}I-IMT via the urinary tracts was observed. The affinity of the parent Tyr to various transport systems, and metabolic pathways, may be changed by altering the structural heterogeneity of artificial amino acids through α-methylation and iodination of the benzene ring.

These results indicate several potential clinical applications 4-^{125}I-*m*Tyr. In the biodistribution study, brain uptake of 4-^{125}I-*m*Tyr was comparable to that of ^{125}I-IMT, suggesting the possibility of brain function imaging. A possible use in pancreas imaging was also indicated because of the relatively high uptake. The properties of 4-^{125}I-*m*Tyr, including rapid clearance from blood, rapid urinary excretion, and relatively low accumulation in kidney, offer advantages for performing abdominal tumor SPECT of areas around the kidney when compared with α-methylated Tyr analogs. A prerequisite for an improved amino acid, such as 4-^{125}I-*m*Tyr, must be that tumor uptake is at least as high but preferably higher than that of ^{123}I-IMT. Further investigation is needed to clarify these points and to develop 4-^{125}I-*m*Tyr as an amino acid transport marker for SPECT.

CONCLUSION

The artificial amino acid 4-^{125}I-*m*Tyr demonstrated high metabolic stability, rapid blood clearance, rapid urinary excretion, and biodistribution similar to that of ^{125}I-IMT. We believe that 4-^{125}I-*m*Tyr is a competitive substrate of L-Tyr reabsorption. However, 4-^{125}I-*m*Tyr possesses different pharmacologic features than ^{125}I-IMT, particularly in renal handling. 4-^{125}I-*m*Tyr may potentially be applied as a new amino acid transport marker. Further investigation is needed to develop 4-^{125}I-*m*Tyr as an amino acid transport marker for SPECT and to clarify its behavior in each target organ and tissue.

ACKNOWLEDGMENTS

The authors thank Shyu-ichi Nakajima, Toshio Miyamoto, and Yuri Aizawa (Ibaraki Prefectural University) for their technical assistance. This work was supported by Grants-in-Aid for Scientific Research (10770451, 14770498, and

13557075) from the Ministry of Education, Science, Sports and Culture of Japan and the Japan Society for the Promotion of Science. Financial support was also provided from the Ibaraki Prefectural University Project Research (grants 9808-3, 0118-1, and 0220-1) and Ibaraki Prefectural University Grants-in-Aid for the Encouragement of Young Scientists 2001 and 2002.

REFERENCES

1. Kawai K, Flores LG II, Nakagawa M, et al. Brain uptake of iodinated L-meta-tyrosine, a metabolically stable amino acid derivative. *Nucl Med Commun.* 1999;20:153–157.
2. Adams ML, Ponce YZ, Berry JM. Synthesis of L-6-[^{123}I]iodo-m-tyrosine: a potential SPECT brain imaging agent. *J Labelled Compds Radiopharm.* 1989; 28:1065–1072.
3. Flores LG II, Kawai K, Nakagawa M, et al. A new radiopharmaceutical for the cerebral dopaminergic presynaptic function: 6-radioiodinated L-*meta*-tyrosine. *J Cereb Blood Flow Metab.* 2000;20:207–212.
4. Hull RN, Cherry WR, Weaver GW. The origin and characteristics of a pig kidney cell strain, LLC-PK$_1$. *In Vitro Cell Dev Biol Anim.* 1976;12:670–677.
5. Saito H, Ohtomo T, Inui K. Na^+-dependent uptake of 1,5-anhydro-D-glucitol via the transport systems for D-glucose and D-mannose in the kidney epithelial cell line, LLC-PK$_1$. *Nippon Jinzo Gakkai Shi.* 1996;38:435–440.
6. Hori R, Yamamoto K, Saito H, Kohno M, Inui K. Effect of aminoglycoside antibiotics on cellular functions of kidney epithelial cell line (LLC-PK$_1$): a model system for aminoglycoside nephrotoxicity. *J Pharmacol Exp Ther.* 1984;230: 742–748.
7. Inui K, Saito H, Hori R. H^+-gradient-dependent active transport of tetraethylammonium cation in apical-membrane vesicles isolated from kidney epithelial cell line LLC-PK$_1$. *Biochem J.* 1985;227:199–203.
8. Inui K, Saito H, Iwata T, Hori R. Aminoglycoside-induced alteration in apical membranes of kidney epithelial cell line (LLC-PK$_1$). *Am J Physiol.* 1988;254: C251–C257.
9. Inui K, Saito H, Takano M, Okano T, Kitazawa S, Hori R. Enzyme activities and sodium-dependent active D-glucose transport in apical membrane vesicles isolated from kidney epithelial cell line (LLC-PK$_1$). *Biochim Biophys Acta.* 1984; 769:514–518.
10. Mullin JM, Fluk L, Kleinzeller A. Basal-lateral transport and transcellular flux of methyl α-D-glucoside across LLC-PK$_1$ renal epithelial cells. *Biochim Biophys Acta.* 1989;885:233–239.
11. Kawai K, Fujibayashi Y, Saji H, et al. A strategy for the study of amino acid transport using iodine 123-labeled amino acid radiopharmaceutical 3-iodo-alpha-methyl-L-tyrosine. *J Nucl Med.* 1991;32:819–824.
12. Kawai K, Fujibayashi Y, Yonekura Y, et al. An artificial amino acid radiopharmaceutical for single photon emission computed tomographic study of pancreatic amino acid transports: ^{123}I-3-iodo-alpha-methyl L-tyrosine. *Ann Nucl Med.* 1992; 6:169–175.
13. Brazeau P. Inhibitors of tubular transport of organic compounds. In: Goodman L, Gilman A, eds. *The Pharmacologic Basis of Therapeutics.* New York, NY: MacMillan Publishing, Inc.; 1975:862–863.
14. Rabito CA, Karish MV. Polarized amino acid transport by an epithelial cell line of renal origin (LLC-PK$_1$): the basolateral systems. *J Biol Chem.* 1982;257:6802–6808.
15. Forster RP, Copenhaver JH. Intracellular accumulation as an active process in a mammalian renal transport system in vitro. *Am J Physiol.* 1956;186:167–171.
16. Rosenberg LE, Blair A, Segal S. Transport of amino acid by slices of rat-kidney cortex. *Biochim Biophys Acta.* 1961;54:479–488.
17. Christensen HN. Role of amino acid transport and counter-transport in nutrition and metabolism. *Physiol Rev.* 1990;70:43–77.
18. Volkow ND, Fowler JS. Neuropsychiatric disorder's investigation of schizophrenia and substance abuse. *Semin Nucl Med.* 1992;22:254–267.
19. Wester HJ, Herz M, Weber W, et al. Synthesis and radiopharmacology of *o*-(2-[^{18}F]fluoroethyl)-L-tyrosine for tumor imaging. *J Nucl Med.* 1999;40:205–212.
20. Inoue T, Tomiyoshi K, Higuichi T, et al. Biodistribution studies on L-3-[fluorine-18]fluoro-α-methyl tyrosine: a potential tumor-detecting agent. *J Nucl Med.* 1998;39:663–667.
21. Langen KJ, Roosen N, Coenen HH, et al. Brain and brain tumor uptake of L-3-[^{123}I]iodo-α-methyl tyrosine: competition with natural L-amino acids. *J Nucl Med.* 1991;32:1225–1228.
22. Langen KJ, Coenen HH, Roosen N, et al. SPECT studies of brain tumors with L-3-[^{123}I]iodo-α-methyl tyrosine: comparison with PET, ^{124}IMT and first clinical results. *J Nucl Med.* 1990;31:281–286.
23. Kloss G, Leven M. Accumulation of radioiodinated tyrosine derivatives in the adrenal medulla and in melanomas. *Eur J Nucl Med.* 1979;4:179–186.
24. Inoue T, Koyama K, Oriuchi N, et al. Detection of malignant tumors: whole-body PET with fluorine 18 a-methyl tyrosine versus FDG: preliminary study. *Radiology.* 2001;220:54–62.
25. Verbruggen AM, Nosco DL, Nerom CG, et al. Technetium-99m-L, L-ethylenedicysteine: a renal imaging agent. I. Labeling and evaluation in animals. *J Nucl Med.* 1992;33:551–557.
26. Kawai K, Shikano N, Nishii R, et al. What kind of membrane transport does 3-[^{123}I]-α-methyl-L-tyrosine mediate in kidney cortex? a new type renal radiopharmaceutical for functional imaging. *J Labelled Compds Radiopharm.* 1999; 42:652–654.
27. Segal S, Their SO. *Handbook of Physiology: Renal Physiology.* Washington, DC: American Physiological Society; 1973.
28. Williams WM, Hang KC. In vitro and in vivo renal tubular transport of tryptophan derivatives. *Am J Physiol.* 1970;219:1468–1475.
29. Williams WM, Hang KC. Structural specificity in the renal tubular transport of tyrosine. *J Pharmacol Exp Ther.* 1981;219:69–74.
30. Palacin M, Estevez R, Bertan J, Zorzano A. Molecular biology of mammalian plasma membrane amino acid transporters. *Physiol Rev.* 1998;76:969–1054.
31. Maenz DD, Patience JF. L-Threonine transport in pig jejunal brush border membrane: functional characterization of the unique system B in the intestinal epithelium. *J Biol Chem.* 1992;267:22079–22086.
32. Lynch AM, McGivan JD. Evidence for a single common Na^+-dependent transporter for alanine, glutamine, leucine and phenylalanine in brush-border membrane vesicles from bovine kidney. *Biochim Biophys Acta.* 1987;899:176–184.
33. International Cystinuria Consortium. Non-type I cystinuria caused by mutations in SLC7 A9, encoding a subunit ($b^{0,+}$ AT) of rBAT. *Nat Genet.* 1999;23:52–57.
34. Jager PL, Vaalburg W, Pruim J, Vries EGE, Langen K-J, Piers DA. Radiolabeled amino acids: basic aspects and clinical applications in oncology. *J Nucl Med.* 2001;42:432–445.